Product Volatilization as a Probe of the Physics and Chemistry of Latent Image Formation in Chemically Amplified Resists[†,‡]

W. D. Hinsberg,*,[§] F. A. Houle,*,[||] G. M. Poliskie, D. Pearson, M. I. Sanchez, and H. Ito

IBM Almaden Research Center, 650 Harry Road, San Jose, California 95120

Received: January 16, 2002

Chemical analyses of vapors desorbing from chemically amplified resist films and kinetic analyses of deprotection, vaporization, and film densification during postexposure thermal processing provide important information on the volatilization of resist components, available decomposition pathways, and mechanistic details of image formation. We have made several types of in situ measurements to characterize imaging chemistry and physics during postexposure bake (PEB). Volatile products from the thermal and acid-catalyzed deprotection of poly(*tert*-butoxycarbonyloxystyrene) (PTBOCST) to form poly(hydroxystyrene) have been identified by mass spectrometry. The results show that two reaction pathways are present with markedly different chemistries and that the generally accepted deprotection mechanism oversimplifies what is actually happening in the film. Using infrared spectroscopy and spectroscopic reflectometry, the relative rates of deprotection, product volatilization, and film densification of PTBOCST homopolymer and copolymer resists during PEB were assessed. These data rule out any significant accumulation of excess free volume or marked plasticization of the resist film during normal PEB, providing evidence against a transient enhancement in acid mobility leading to image blur mediated by these factors.

Introduction

In essentially all positive-tone chemically amplified (CA) resists, post apply bake (PAB), exposure, and postexposure bake (PEB) process steps involve desorption of small molecules from the polymeric film.[1,2] These species can be impurities, solvents, photolysis, and thermolysis products. The particular case of PEB is illustrated in Figure 1. Primary deprotection products generated during bake can undergo secondary reactions with other components of the film, including the polymer, photogenerated acid if present, and other small molecules.[3] The volatile species resulting from these reactions will, in turn, be emitted from the film, leading to a decrease in film mass and thickness loss due to densification. Analyses of the structures and distributions of the deprotection products and of the time evolution of their formation and volatilization can reveal detailed mechanistic information about the complex processes underway during PEB. Of particular interest is the interplay between the deprotection kinetics and the polymeric environment, as the latter has a profound effect on mobility in the resist, directly influencing the image formation process.

The mobilities of diffusant molecules can be influenced by numerous factors that include permeant size, shape, and charge; polymer and permeant polarities; and the amount of excess free volume.[4] In solid polymers, diffusive motion is usually considered to occur by a series of hops when the local free volume around a diffusing molecule exceeds a certain critical value. The probability of finding sufficient free volume is related to the total free volume of the film. Ionic diffusion in polymers is considered in similar terms, as a hopping process dominated by dynamic fluctuations in local density of the polymer host.[5] It was recognized some time ago that, depending on the relative rates of deprotection, volatiles evolution, and film densification, transient excess free volume could be present in CA resist films during PEB, potentially playing a role in mediating acid transport.[6] Dissolved molecules whose melting/glass transition temperatures are below the PEB temperature could potentially act as plasticizing agents, which are considered to effectively increase the free volume of the polymer film.[7] Therefore, a transient accumulation of the deprotection products in a CA resist film during PEB might also be anticipated to enhance acid mobility. Recently such effects have been invoked to rationalize the deprotection kinetics measured for a multilayer thin-film test structure and have been proposed to control image blurring in CA resists.[8,9] This model is an alternative to the reaction−diffusion mechanism that has emerged from direct kinetics studies in which experimental data are reproduced by considering only changes in polymer composition, not transient morphologies.[10,11] In the present work, we seek to distinguish between these models by obtaining direct experimental evidence for product accumulation and/or excess free volume in a well-defined CA resist system.[12]

We describe the application of several spectrometric techniques to probe the details of volatiles formation during the processing of resist materials. The resist systems chosen are formulated using (1) poly(*tert*-butoxycarbonyloxystyrene) (PTBOCST), which deprotects to form poly(hydroxystyrene) (PHOST), and (2) a 39:61 TBOC/HOST copolymer. Many aspects of the chemistry of PTBOCST deprotection have been studied in great detail, primarily using spectroscopic probes of the films such as visible and infrared spectroscopies and thermal analysis[13] or NMR spectroscopy.[3] It is generally assumed that the chemistry of PTBOCST deprotection is loss of CO_2 and

[†] Part of the special issue "Jack Beauchamp Festschrift".

[‡] This paper is dedicated to Professor J. L. Beauchamp in honor of his 60th birthday, with gratitude for teaching me to see the frontiers (F.H.).

* To whom correspondence should be addressed.

[§] E-mail: hnsbrg@almaden.ibm.com.

[||] E-mail: houle@almaden.ibm.com.

10.1021/jp0201332 CCC: $22.00
Published on Web 08/15/2002

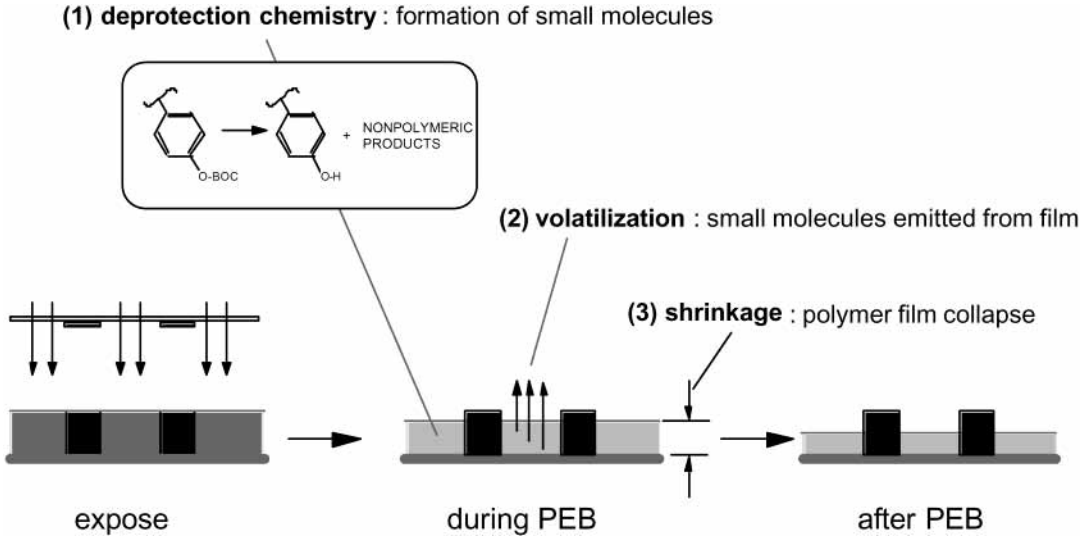

Figure 1. Sequential steps during postexposure bake of a chemically amplified resist.

isobutylene to form PHOST, during both the simple thermolysis and the thermally activated acid-catalyzed reaction occurring after exposure[14]

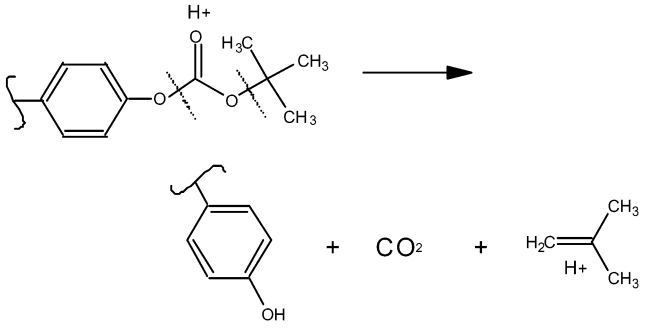

There have been no direct measurements of volatile products, however, although some related data are available for methacrylates.[15] Upon complete deprotection, the molar density of a film of PTBOCST polymer increases by 50% and its mass decreases by about 45%. The corresponding changes in the copolymer are an increase of 12% and a decrease of 25%, respectively.[13,16] These are extreme changes by the standards used to design current resist chemistries and should readily display any effects stemming from the transient accumulation of deprotection products or the presence of transient excess free volume during PEB processing. We have investigated both the film and the desorbing vapors during PEB. Direct atmospheric-pressure mass spectrometric analysis of vapors emitted from CA resist films and polymer powders are used to characterize the reaction pathways that are active during deprotection and the relative abundances of small-molecule products. In situ kinetic analyses of resist film composition and structure during PEB using infrared spectroscopy and spectroscopic reflectometry allow a comparison of the rates of deprotection, volatiles evolution, and film densification.[17]

Experimental Section

Materials. TBOCST monomer was obtained from Eastman Kodak. Resists were formulated using PTBOCST polymer or a 39:61 TBOC/HOST copolymer. PTBOCST polymer was obtained from Eastman Kodak, and the copolymer was prepared as described elsewhere.[18] PHOST was obtained from Hoechst-Celanese (now TriQuest). Di-*tert*-butylphenyl iodonium trifluoromethanesulfonate (TBI-T) and di-*tert*-butylphenyliodonium perfluorobutanesulfonate (TBI-PFBS) were used as photoacid generators (PAGs). The kinetics of deprotection are essentially identical for the two PAGs (although their diffusion rates are very different), enabling data for blanket-exposed films containing them to be compared directly. Excepting samples prepared for reflectance spectroscopy, films were cast from propylene glycol methyl ether acetate (PGMEA) solutions onto cleaned Si wafers coated with 100 nm of a bottom antireflection layer (BARL 900, IBM, East Fishkill, NY). Additional details of the resists and of film preparation procedures are given in ref 10. Porous poly(methylsilsesquioxane) (PMSSQ) films were prepared as described in ref 19 and used as controls for reflectance spectrometry.

Exposures. Films were exposed at 254 nm using an Optical Associates Incorporated (OAI) deep ultraviolet (DUV) lamp. The light intensity at the wafer plane was measured using a calibrated exposure monitor (OAI 355 or P354) and a 254-nm probe.

Mass Spectrometer. Mass spectrometry (MS) is the analytical method of choice for in situ identification of gas-phase reaction products. However, it requires high vacuum, the ionization process can complicate the analysis because of extensive fragmentation, and the unique identification of components of mixtures can be difficult. Atmospheric-pressure chemical ionization (APCI) sources coupled to well-designed vacuum systems overcome these difficulties and are in widespread use for trace component analysis.[20] In this work, we have adapted a Sciex trace atmospheric gas analyzer (TAGA) 6000 E triple quadrupole mass spectrometer for resist outgassing studies.[21] The instrument is designed for direct, on-the-fly sampling of high-pressure gas streams and can be operated in single-mass filter or one of several MS−MS modes. The APCI source is a needle biased to several kilovolts in a chamber at atmospheric pressure, forming a corona of positively and negatively charged species. The majority of these species are water ion clusters, which effect soft ionization through electron, hydride, and proton transfer. APCI offers advantages for the analysis of complex gas mixtures, including low spectral congestion, and minimal fragmentation on ionization, both of which enable part-per-billion sensitivity. The accumulated spectral data can provide product identity and, under appropriate conditions, the product formation timeline in a single experiment. Species that have a proton affinity lower than that of

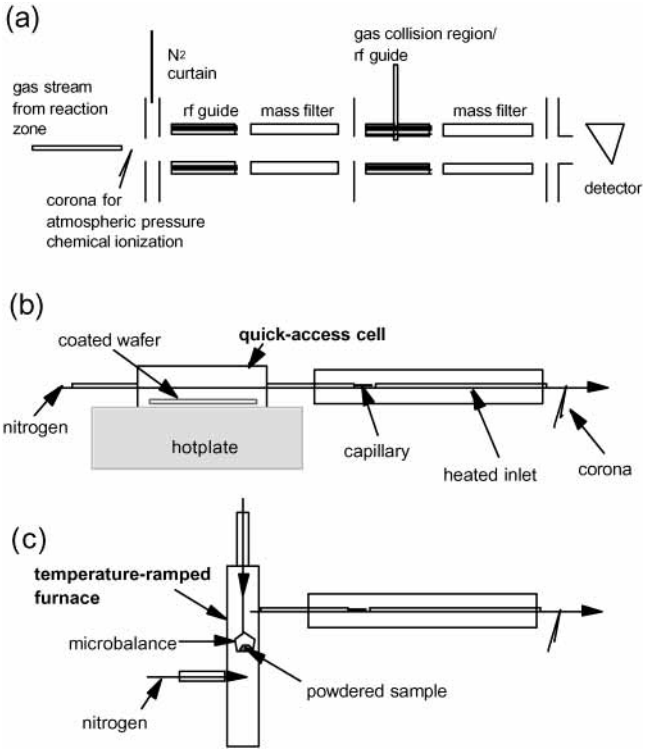

Figure 2. Schematic of mass spectrometer and inlet sources: (a) mass spectrometer, (b) isothermal cell coupled to inlet gas stream, (c) thermogravimetric analyzer coupled to inlet gas stream.

water, such as nitrogen, CO_2, alkanes and rare gases, cannot be detected, and relative sensitivities among functional groups are dependent on proton-transfer kinetics.[22] Sensitivities are comparable for similar functional groups,[23] and we assume that chemically similar products have similar sensitivities, allowing a qualitative estimate of branching ratios between major paths to be made.

Our instrument is interfaced to one of two sample sources, as illustrated in Figure 2: a Perkin-Elmer TGS-2 thermogravimetric analyzer (TGA) for analysis of bulk samples (powders, liquids, or scraped films) following a predefined temperature program or a fast-access, isothermal hotplate cell for direct studies of spin-cast thin films. The Thermodyne 1900 hotplate is controlled by an Omega CN 76000 temperature regulator with a K-type thermocouple feedback and is temperature-stabilized to within 0.1 °C. The cell is equipped with a vacuum chuck to ensure good thermal contact between the wafer and the baseplate. It uses a vacuum-sealed lid to allow opening, loading and closing of the cell within 2−3 s to avoid loss of data. Gas-phase reaction products are sampled using a stream of ultrapure nitrogen flowing through the enclosed reaction zone. The products pass through an all-glass line that uses a high-flow gas stream to extract a small fraction of the product gases through a capillary for analysis. This arrangement ensures that, from the capillary on, there are no collisions between analyte species and minimal wall interactions.

The spectrometer is set to scan repetitively over a mass range while the experiment proceeds, providing a complete time history for all products. These time-dependent data must be interpreted cautiously, with the following points kept in mind: (1) migration of products through the film and subsequent desorption might not occur at a uniform rate for all species; (2) only products that have significant volatilities are observed; (3) product intensities depend on both the gas-phase concentration of the analyte and the proton-transfer kinetics; and (4) sharp transients can be missed because of the relatively slow scan rate that must be used (approximately 30 ms/amu) to allow the fields inside the mass spectrometer to settle. The raw data presented here cannot be used to determine absolute product distributions without calibration for absolute sensitivities and for extent of mass discrimination,[24] a complex task made particularly challenging by the number of products observed. It is straightforward to measure sensitivities for various compound types, however. Using a syringe pump to deliver controlled doses, order-of-magnitude relative sensitivities for ketones, alcohols, and alkenes, the primary resist deprotection product types, are estimated to be 2:1:1 for steady flow and 100:1:1 for transient (<1-s injection time) loads when the amounts of materials are held constant. Thus, the sensitivity to ketones will depend on whether the products desorb in a rapid burst or slowly during deprotection. The variability of the ketone signal depending on injection mode results from the kinetics of the interactions of the analyte gas with the glass inlet line walls in the region before and in the sampling capillary.

Several types of measurements were made. Simultaneous MS and TGA of pure PTBOCST and TBOC/HOST polymer powders and of TBOCST monomer were obtained over a temperature range of 40−300 °C. Heating rates of 5 and 20 °C/min were used. Volatiles emitted during wafer processing were observed using the fast-access cell. Spectra were obtained during PAB at 110 °C of ca. 1000-nm-thick PTBOCST films with TBI-T PAG cast onto Si. To avoid overloading the mass spectrometer, the casting solvent was allowed to evaporate out of the films for a period of several days while the wafers were stored in the dark. Data were also acquired during PEB at about 100 °C for PTBOCST/TBI-T films exposed with 254-nm light after 90 s PAB at 130 °C to doses of 0.5 and 100 mJ/cm^2. Although most of the important ions could be assigned by inspection, in some cases, mass assignments were made by using MS−MS techniques to fragment selected ions and identify their structures.[25]

Infrared Spectroscopy. Infrared spectra were acquired using a Nicolet Continuum infrared microscope attached to a Nicolet Nexus 470 Fourier transform infrared spectrometer or a Nicolet IR/44 Fourier transform infrared spectrometer. IR kinetic analyses were carried out using a standard protocol described in earlier work.[10,13]

Reflectance Spectroscopy. The changing reflectivity characteristics of a thin CA resist film during PEB allows for the extraction of information on both its instantaneous film thickness and its refractive index. From these data, in turn, rates of volatilization and film densification can be derived. The theory of thin-film reflectivity is well-established, and precise quantitative methods for the calculation and analysis of optical properties of even very complex thin-film structures have been available for many years.[26] Thin-film reflectivity analysis using visible light is well-suited for the measurement of films with thicknesses on the order of ca. 3 μm and below, so this technique is in wide use by the semiconductor industry for process and quality control.

Reflectivity measurements were carried out using a high-speed CCD-based spectroscopic reflectometer (model HSDRM, SC Technologies, Fremont, CA) specially modified to facilitate reflectance measurements of substrates placed on a heated copper block (Figure 3). A Fostec model DCRII broad-band quartz/halogen light source (500 nm < λ < 800 nm) projects an illuminated strip onto the wafer under study. An image of that strip is dispersed by a grating onto the sensor of a high-speed CCD camera. The detector optics are configured such

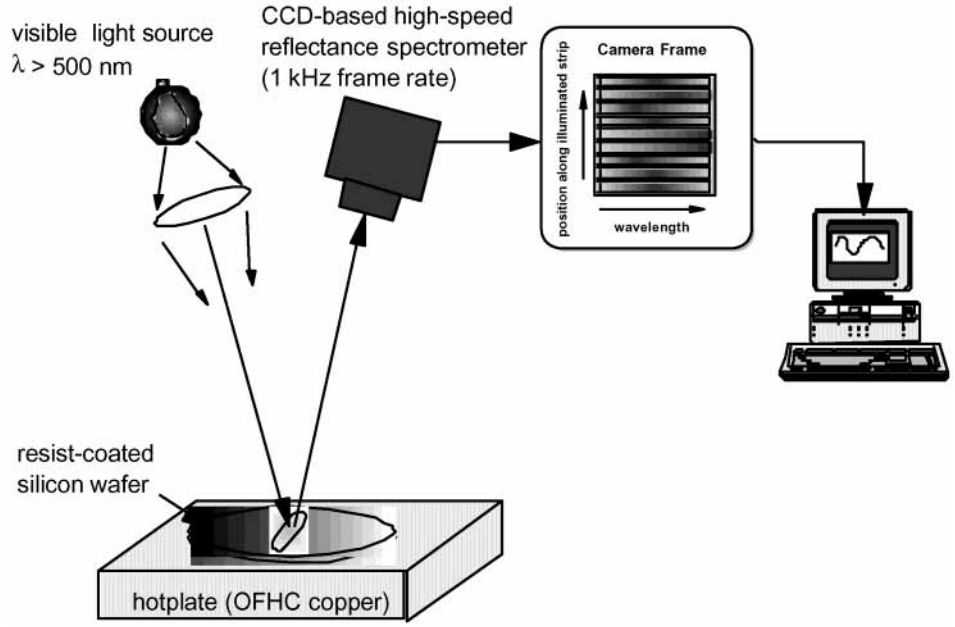

Figure 3. Schematic diagram of the spectroscopic reflectometer used in this work.

that each row of pixels senses light reflected from a different position along the illuminated strip, while each column of pixels is illuminated by a different wavelength. The result is that each image frame captured by the camera represents a collection of reflectance spectra, each corresponding to a different position along the length of the illuminated strip. In a typical experiment, the camera is first initialized and begins storing image frames at a predetermined rate (up to 1000 frames/s). An exposed resist film, coated on a 1-in.-diameter silicon wafer, is then placed on the heated block. Following the completion of the experimental run, each stored frame is read out and corrected for dark count and for nonuniformities in illumination and individual pixel response, adjacent rows are binned into groups of six to improve the signal-to-noise ratio, and the absolute reflectances that result are saved along with the elapsed time for each frame. These reflectance spectra are analyzed further using SC Technologies Inspector 800 software or in-house software based on the Berning and Berning algorithms.[27]

Method for Measurement of Free Volume by Spectroscopic Reflectometry. The visible reflectivity of smooth, thin transparent films is dominated by optical interference. The absolute reflectance R is determined by materials properties (the wavelength-dependent complex refractive indices of the incident medium, the film, and the substrate and the film thickness), and by the polarization, angle of incidence, and wavelength of the interrogating light beam. A comparison of experimental values of R, measured at multiple wavelengths, with those predicted by optical theory allows the thickness and optical constants of the thin film to be estimated when all other parameters are known.[28] Spectroscopic reflectometry has been applied to the characterization of resist dissolution[29,30] and for the monitoring of solvent removal during PAB of DNQ/novolac resists.[31] Figure 4 provides an illustration of how polymer film characteristics influence reflectivity. Figure 4a displays calculated reflectance spectra for a range of film thicknesses of a 1:1 TBOCST/HOST copolymer. A small change in film thickness leads to a significant change in the form of the reflectance spectrum. In practice, film thickness changes of less than 1 nm can be readily discerned. This family of curves highlights a useful property: for a given material, the extrema of the reflectance spectra will always fall along two curves (shown as dotted lines on each graph) whose forms are determined by the optical constants of the incident medium, the substrate, and the thin film. Figure 4b displays reflectance spectra for two films of different composition (PTBOCST and PHOST) but identical 1000-nm thickness. The two polymers differ in refractive index, leading to changes in the wavelengths at which the extrema are located. For both materials, the maxima fall along the same limiting curve, but the values for the reflectances at the minima do not. This latter difference illustrates a second useful property: the maximum reflectance is independent of the optical constants of the film (in fact, it is equal to the reflectance of the uncoated substrate), while the minimum reflectance depends in a well-defined way on the refractive index of the film. By design, a CA resist film changes in composition during PEB, which modifies its refractive index; in our work, this change is taken into account by applying an effective medium approximation (EMA)[32,33] to model the refractive indices of intermediate polymer compositions.

Figure 4c shows calculated reflectance spectra for 1000-nm films of 1:1 TBOCST/HOST copolymer containing increasing amounts of excess free volume. An EMA is used to model the optical constants of these films. Here, the presence of excess free volume is signaled by a vertical offset in the reflectance minima from the curve predicted with the optical constants of the densified material, and the amount of free volume is directly related to the magnitude of the offset. Figure 4d presents experimental data that illustrate this effect for a different system. Shown are reflectance spectra of cured films of poly(methylsilsesquioxane) (PMSSQ),[19] one of which was formulated with 25% added porogen that, during cure, produces pores with dimensions much smaller than visible wavelengths throughout the film. The other film was prepared from a formulation that contained no porogen and, hence, yielded a nonporous film upon cure. The porous film displays a minimum reflectance (at 600 nm) with a substantial vertical offset from the limiting curve. From the magnitude of this offset, a void volume of ca. 19% is estimated, consistent with that expected from the initial porogen loading.

Kinetics Simulations. Chemical Kinetics Simulator (CKS)[34] was used to calculate time-dependent compositions and thicknesses of films during deprotection of the PTBOCST resist for

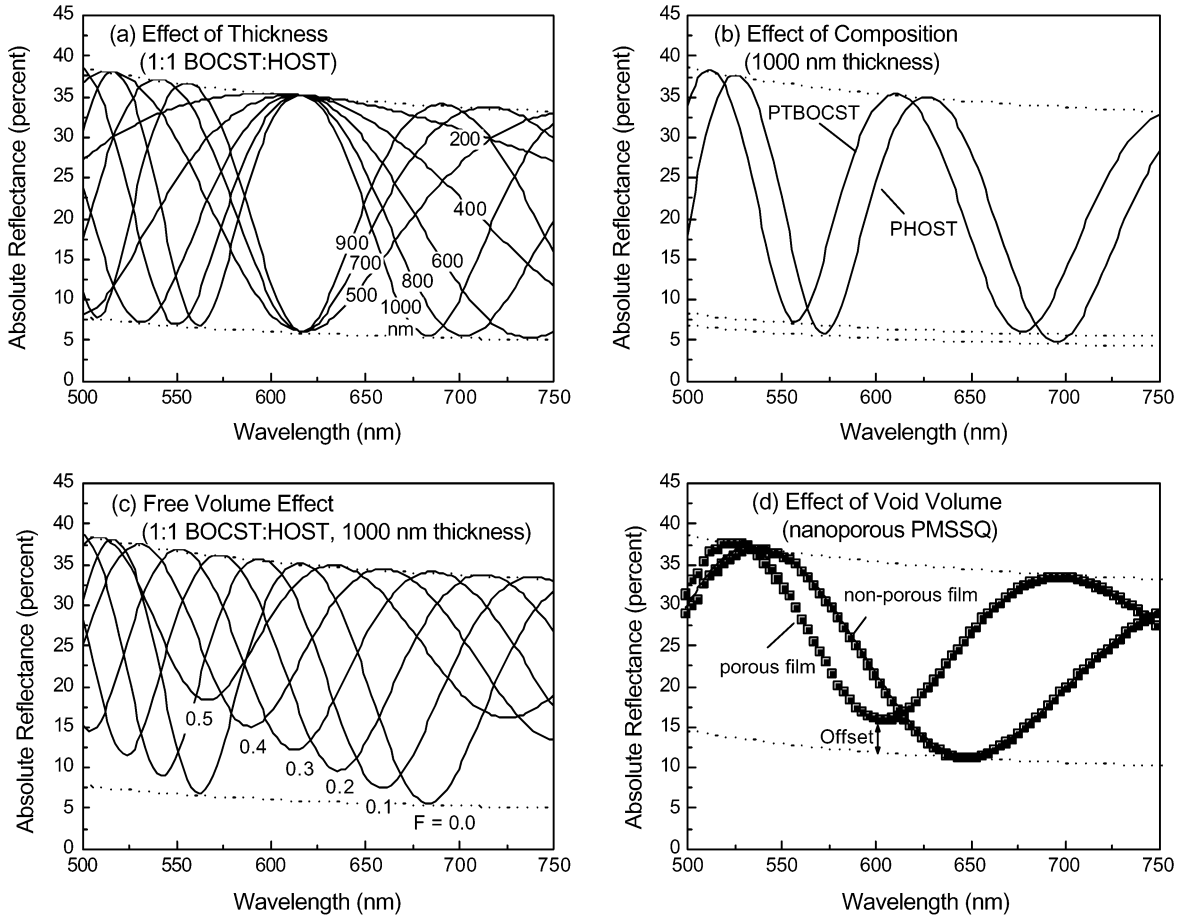

Figure 4. Illustration of the influence of polymer film properties on the absolute reflectance *R* of a coated silicon substrate in the visible wavelength region. The curves in a−c are calculated from optical theory assuming unpolarized light at normal incidence and using experimentally measured values for material optical properties. In each graph the dotted lines represent the extremum values for *R*. Graph a illustrates the effect of film thickness on *R* for a 1:1 TBOCST:HOST copolymer, graph b illustrates the effect of polymer composition on *R* for 1000-nm-thick films of PTBOCST and PHOST homopolymers, graph c shows the effect of excess free volume on *R* for a 1:1 TBOCST/HOST copolymer resist, and graph d presents experimentally measured values of *R* for films of PMSSQ prepared with and without nanoporosity to simulate the effect of free volume. The solid line (in quantitative agreement with experiment) represents the values of *R* calculated for a nonporous PMSSQ film of thickness 584 nm.

comparison to experiment. The kinetics model and rate constants were determined previously.[10,13]

Results

Deprotection of PTBOCST. In all cases—polymer and monomer, simple thermolysis in the TGA, PAB, and PEB—significant numbers of vapor-phase species were observed. Data are presented in Figures 5−7 and Tables 1 and 2. A detailed determination of product identities makes clear that both uncatalyzed and acid-catalyzed deprotection of PTBOCST polymer are more complex than the simple chemistry depicted in the Introduction.

The polymer products were found to be very sensitive to the temperature ramp, with faster ramps producing much more congested spectra than slower ramps. Typical data are shown in Figures 5 and 6. When the temperature is increased quickly (Figure 5), the abrupt nature of the deprotection[13] produces large quantities of small molecules in a short time span. The concentrations of reactive intermediates are high enough to promote numerous secondary reactions during the residence time of the products in the solid. As seen in Figure 6, a temperature ramp of 5 °C/min minimizes the product evolution rate, and hence the secondary chemistry, and facilitates interpretation of the data.

Although isobutylene is a major component of the volatile product mix, a large number of other species can be identified. Some of these structures are products expected of secondary reactions of a *tert*-butyl intermediate (for example, 3-methylene-1-butene, seen at *m*/*e* 69). Other major products are species whose formation is difficult to rationalize solely on the basis of fragmentation to produce a *tert*-butyl intermediate (presumably a free radical during uncatalyzed thermolysis or a cation in the presence of an acid catalyst). For example, as shown in Table 1 our PAB results indicate that the lowest-energy decomposition pathway in an unexposed PTBOCST/TBIT film upon heating at 129 °C is cleavage of the O−C═O bond to form an alkoxy radical that subsequently decomposes to form acetone (*m*/*e* 59), which is seen in equilibrium with its hydrate (*m*/*e* 77). Data are presented in Figure 7a. These are well-known reactions that are a signature for the *tert*-butoxy species.[35] TGA experiments show that the *tert*-butoxy decomposition pathway accounts for about 3% of the total mass loss up to a temperature of 175 °C. Above that temperature, a new channel opens: loss of *tert*-butyl radical, accompanied by the formation of a number of secondary reaction products, including methyl isopropenyl ether (*m*/*e* 73) and small amounts of *tert*-butyl alchohol (*m*/*e* 75), which presumably are derived from *tert*-butoxy radical (see Figures 5 and 6). Data comparing the evolution of the *m*/*e* 57 and *m*/*e* 59 signals are shown in Figure 7b.

These results are in contrast to the thermal decomposition of the TBOCST monomer, which involves the isobutylene channel exclusively, as presented in Figure 8. It appears that the

TABLE 1: Species Observed during Thermal Decomposition of TBOCST Monomer, PTBOCST, and TBOCST-HOST Copolymer

ion m/e[a]	proposed assignment of parent structure	TGA[b] TBOCST monomer 155 °C 20 °C/min	TGA TBOCST polymer 210 °C 5 °C/min	isothermal TBOCST polymer/ TBI-T 109 °C	isothermal TBOCST polymer/ TBI-T 129 °C
41	propyne		0.07		
43	propylene, ketene		0.02		
57	**isobutylene**	**0.17**	**0.35**		
59	**acetone**		**0.19**	**0.48**	**0.5**
69	**3-methylene-1-butene**		**0.1**		
73	**methyl isopropenyl ether**		**0.14**		
75	***tert*-butyl alcohol**		0.03		
77	**acetone hydrate**			**0.41**	**0.35**
81	C_5H_5O	0.03			
91	$C_4H_{10}O_2$	0.01	0.02		
93	$C_3H_8O_3$		0.02		
95	C_7H_{10}		0.04		
107	C_7H_7O, C_8H_{11}	0.06			
110	$C_6H_{11}CN$		0.02		
117	**$C_5H_8O_3$, $C_6H_{12}O_2$**			0.08	**0.1**
121	**hydroxystyrene**	**0.21**			
133	PGMEA			0.02	0.02
151	**$C_9H_{11}O_2$**	**0.1**			
165	**$C_9H_9O_3$**	**0.2**			
221	**TBOC monomer**	**0.19**			0.02

[a] Masses are for the protonated neutral. Major species are highlighted in bold type. Intensities are normalized to the total ion signal for each measurement and are uncorrected for TAGA sensitivity. Water ions and small background peaks have been subtracted. [b] TGA ramps are from 40 to 300 °C. The reported spectra are for the temperatures at which the decomposition rate reaches a maximum.

TABLE 2: Species Observed during Acid-Catalyzed Deprotection of PTBOCST

ion m/e[a]	proposed assignment of parent structure[b]	PEB 101 °C TBOCST polymer/ TBI-T 0.5 mJ/cm^2	PEB 103 °C TBOCST polymer/ TBI-T 100 mJ/cm^2
29	ethylene	0.01	0.02
41	propyne	0.03	0.05
43	propylene, ketene	0.01	0.02
57	**isobutylene**	**0.29**	**0.17**
59	**acetone**	0.09	**0.14**
61	2-propanol		0.02
69	3-methylene-1-butene	0.03	0.04
71	2-methyl-2-butene	0.03	0.02
73	**methyl isopropenyl ether**	0.05	**0.1**
75	***tert*-butyl alcohol**	0.09	**0.13**
77	acetone hydrate		0.03
85	3,3-dimethyl-1-butene	0.03	0.02
93	**$C_3H_8O_3$**	0.07	**0.11**
95	**C_7H_{10}**	**0.1**	0.06
110	$C_6H_{11}CN$	0.06	0.02
113	2,4,4-trimethyl-1-pentene	0.04	0.02
133	PGMEA	0.01	0.02
142	$C_7H_{14}OCN$	0.04	0.02
149	$C_9H_9O_2$	0.01	
165	$C_9H_9O_3$	0.02	

[a] Masses are for the protonated neutral. Major species are highlighted in bold type. Intensities are normalized to the total ion signal for each measurement and are uncorrected for TAGA sensitivity. Water ions and small background peaks have been subtracted. [b] Based on MS and MS/MS data.

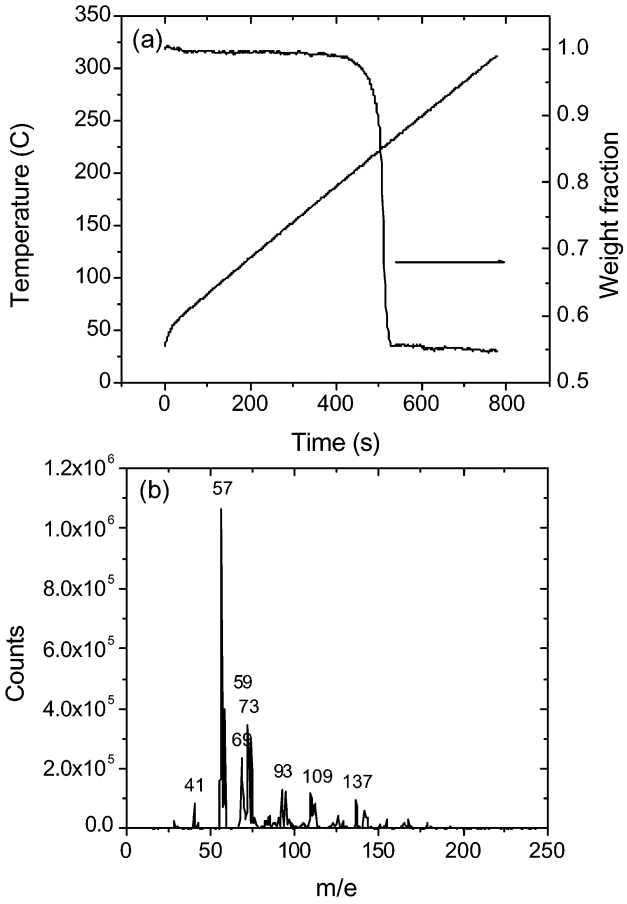

Figure 5. Data for PTBOCST decomposition during heating with a 20 °C/min ramp: (a) TGA data, (b) mass spectrum recorded at the time of the maximum decomposition rate (approximately 500 s).

condensation of the monomer into a polymer opens up significant new deprotection chemistry that had not been recognized previously. This suggests that the use of monomer chemistry to model polymer chemistry should be done with great care.

The product distributions formed by acid-catalyzed reaction during PEB are significantly different from the distribution of thermal products, as shown in Figure 9, and are dose-dependent, as seen in Table 2. At low dose, although the *tert*-butoxy formation channel is still open, deprotection is dominated by the *tert*-butyl product channel. Isobutylene is not the sole

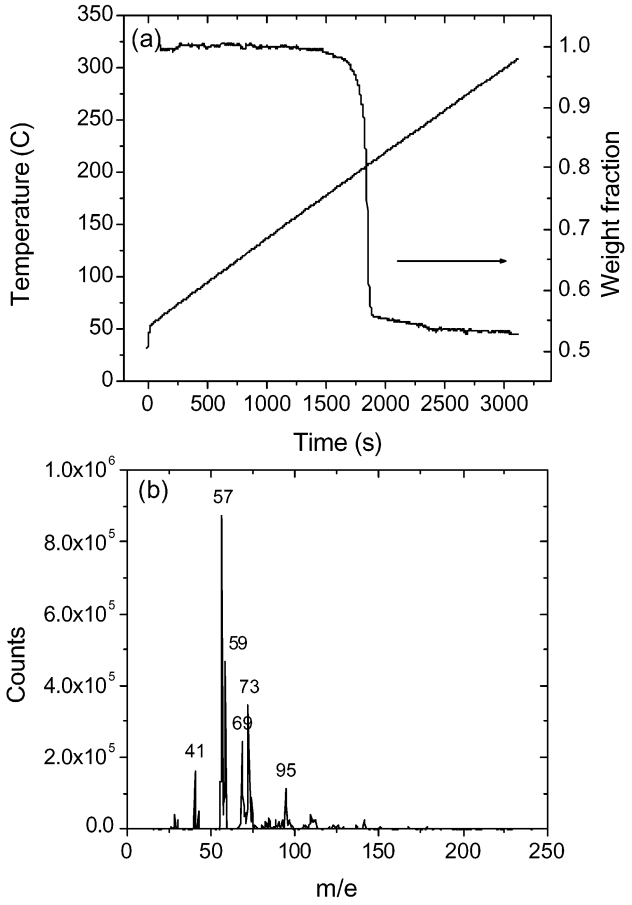

Figure 6. Data for PTBOCST decomposition during heating with a 5 °C/min ramp: (a) TGA data, (b) mass spectrum recorded at the time of the maximum decomposition rate (approximately 1750 s).

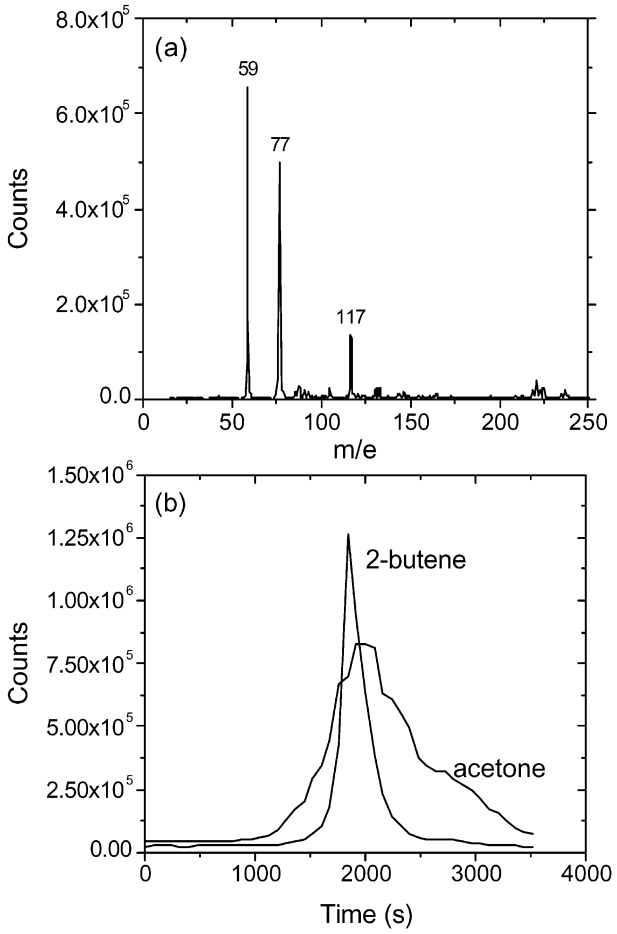

Figure 7. Data showing relative temperature dependences of alkoxy and alkyl decomposition channels: (a) products formed during PAB of PTBOCST/TBI-T resist at 129 °C, 90 s after placement on the hot plate, (b) time-dependent signals taken from the mass spectra recorded during the TGA measurements shown in Figure 6, showing that acetone formation is the low-temperature decomposition channel. The integrated signals for the products give acetone/2-butene $\approx$ 2. The relative sensitivities of the products are about 2:1, so the branching ratio for the formation of the products is about 1 under these conditions.

reaction product; numerous small molecules are observed and account for most of the weight loss from the polymer. The primary side products formed from *tert*-butoxy now include much larger amounts of *tert*-butyl alcohol relative to acetone, resulting from a reaction known to be favored in an environment rich in allylic hydrogens such as are provided by isobutylene. At higher dose, however, both the *tert*-butyl and the *tert*-butoxy channels become more competitive. The overall trend is that an increasing deprotection rate, driven either by increased dose or increased bake temperature, favors the alkoxy decomposition channel. Figure 10 summarizes the two competing acid-catalyzed deprotection pathways.

Relative Rates of Deprotection, Volatiles Evolution, and Film Densification. To probe the dynamic response of the resist film to the formation of these products during deprotection, we have measured, using IR spectroscopy, the time-dependent extent of reaction of exposed films of PTBOCST resist during PEB and, in parallel experiments under identical conditions, changes in the optical properties of these films by spectroscopic reflectometry. These experiments provide, respectively, independent time histories of the evolving film composition and changes in the film thickness and refractive index during PEB. Figure 11 displays the results of one such experiment, carried out at 65 °C on a 1131-nm-thick film of PTBOCST/TBI-PFBS exposed to a dose of 200 mJ/cm^2 at 254 nm. Because of the high dose, essentially all of the TBI-PFBS is photolyzed, providing a uniform acid concentration through the film. For direct comparison, the results of the measurements are plotted in normalized form, showing the fraction deprotected, or the fraction of overall film loss, as a function of time. It is clear that the deprotection chemistry and the thickness loss track precisely. Any significant accumulation of small-molecule deprotection products would be expected to produce a time lag or offset in the film thickness loss relative to the extent of deprotection. These data provide definitive evidence that the volatilization of deprotection products is rapid compared to the rate of deprotection and that there is no substantial accumulation of deprotection products. The figure also includes results of simulations using our previously determined kinetics model,[10,13] which are seen to be in excellent quantitative agreement with the experimental data.

A closer examination of the individual reflectance spectra provides further information. Figure 12 compares a selection of the reflectance spectra recorded during this experiment with those predicted from the instantaneous extents of deprotection that were determined by IR spectroscopy. For the predicted spectra, it was assumed that product volatilization and film densification are rapid compared to deprotection. Agreement between experiment and prediction is excellent. In particular, the reflectance values at the minima of the experimental curves coincide with the positions of the predicted curves, showing a gradual drop from the curve defining the PTBOCST lower limit to the PHOST lower limit as deprotection proceeds. The absence

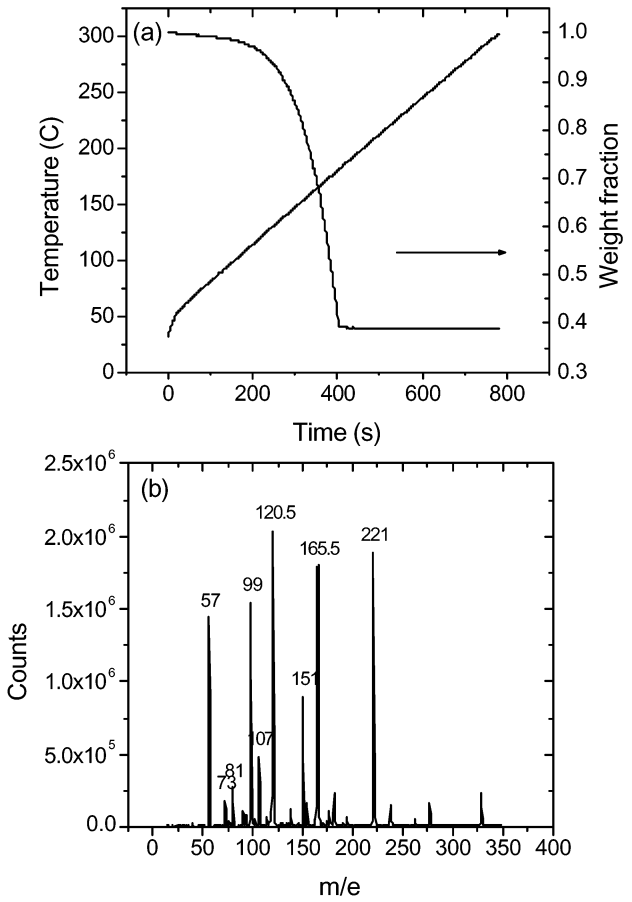

Figure 8. Data for TBOCST monomer decomposition during heating with a 20 °C/min ramp: (a) TGA data, (b) mass spectrum recorded at the time of the maximum decomposition rate (approximately 300 s).

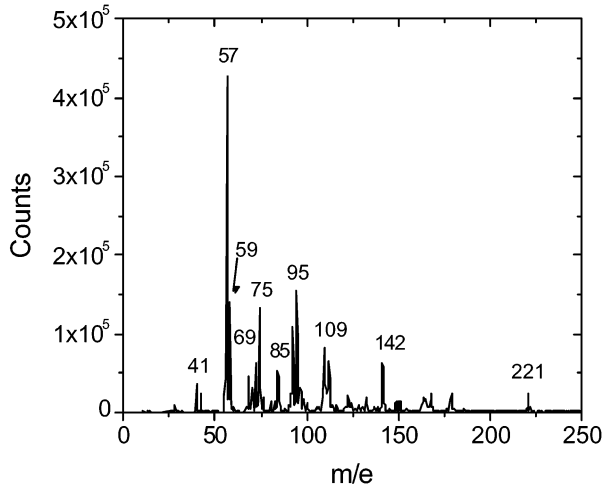

Figure 9. PEB products from PTBOCST/TBI-T resist 90 s after wafer loading, 101 °C bake temperature, 0.5 mJ/cm^2 dose.

of any offsets is an indicator that the material refractive indices, and hence the film densities at each instant during PEB, are in agreement with those predicted solely by consideration of the extent of deprotection. This is evidence that the film densification in this instance is rapid compared to the rate of deprotection and that there is no significant excess free volume (<1% based on an estimate of our detection limit) present during this PEB process.

Whereas the IR kinetic analysis is limited by its relatively slow data acquisition, the high data rate of our reflectometer allows us to extend the reflectance analysis to more extreme process conditions. An analysis of those reflectance data provides information on the rate of film loss and the amount of excess free volume. Table 3 summarizes the results for a range of process conditions. To probe how polymer structure might influence film dynamics, a 39:61 TBOCST/HOST copolymer-based resist was included in this survey, baked at its standard PEB temperature of 85 °C. Under most process conditions (exposure dose and PEB temperature), including those used for normal lithographic imaging of these resist compositions, we find no evidence for the presence of significant transient excess free volume: experimental reflectance spectra match those predicted assuming no excess free volume. Under certain extreme conditions, well outside the useful PEB parameter space, slight transient deviations in the reflectance spectra can be discerned. For example, exposure of the PTBOCST resist formulation to a 200 mJ/cm^2 dose followed by PEB at 100 °C leads to film thickness loss with an effective half-life of 0.5 s. Under these accelerated conditions, minima in the recorded reflectance spectra display a slight offset from predicted values; the offset develops during PEB but disappears by the time the overall film thickness decrease due to densification is substantially complete. Although other factors such as minor nonuniformities in film thickness loss during deprotection cannot be ruled out as the origin of this offset, one possible source is a short-lived decrease in film density due to rapid volatilization of deprotection products, followed by somewhat slower film redensification. If we assume this to be the cause of the offset, then its magnitude is consistent with the intermediate formation and disappearance of ~3% excess free volume during PEB.

Because the rates of each of the sequential steps leading to thickness loss—deprotection, volatilization, and densification—can be no slower than the overall observed rate of densification, the data in Table 3 provide a lower limit for the rates of volatilization and film densification at 100 °C. Reducing the exposure dose to levels normally used to lithographically image PTBOCST (~1−2 mJ/cm^2) leads to a reduction by a factor of 16 or more in the rate of thickness decrease. The effect of a dose reduction is to decrease the acid concentration in the film, and thereby the rate of deprotection chemistry, but it would not be expected to change the inherent time scales of volatilization and film densification, which are probably zeroth-order in acid. We can therefore associate the 16-fold overall rate reduction with a decrease in the rate of chemical deprotection and conclude that, under normal processing conditions, volatilization of the deprotection products and densification of the film occur more than an order of magnitude more rapidly than deprotection.

IR Analysis of PTBOCST Films. The abundance of small reactive molecules formed during deprotection cannot be expected to desorb from the film without interaction with the polymer. As illustrated in Figure 13, several polymeric side products have been identified by NMR spectroscopy in PTBOCST following PEB processing.[3] Infrared spectra for films exposed to 200 mJ/cm^2 doses, baked and unbaked, and for authentic PHOST are compared in Figure 13. The absorption at 2990 cm^{-1} is attributable to the *tert*-butyl group. If this film were to undergo deprotection to generate PHOST as the sole nonvolatile product, then after PEB, the *tert*-butyl absorption should disappear, and its spectrum should essentially match that of pure PHOST. Although the IR spectrum of deprotected PTBOCST does correspond in large part to that of authentic PHOST, it contains an additional absorption band at ca. 2955 cm^{-1} that can be ascribed to the formation of one or more

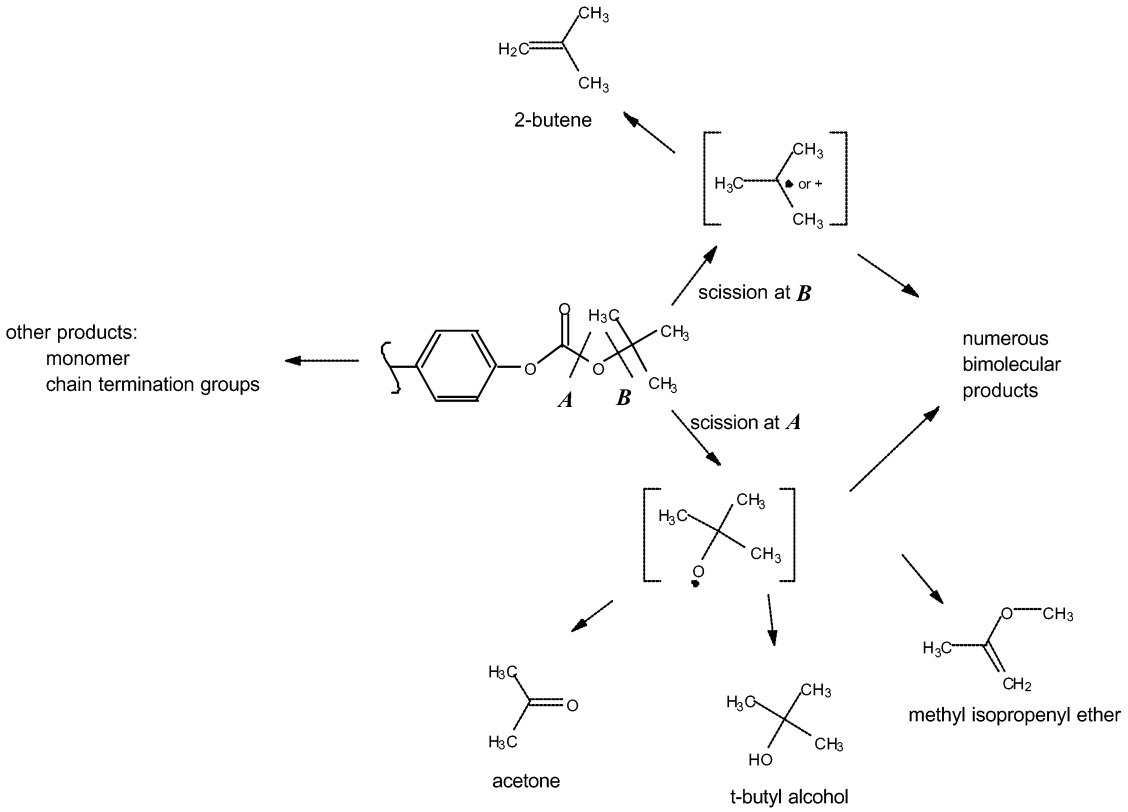

Figure 10. Summary of volatile products detected by TAGA analysis during thermal processing of exposed PTBOCST resist formulations. The products detected are consistent with the presence of *tert*-butyl and *tert*-butoxy reactive intermediates. At low dose, the alkyl/alkoxy branching ratio is about 2.4:1; at high dose, it is about 1:1.

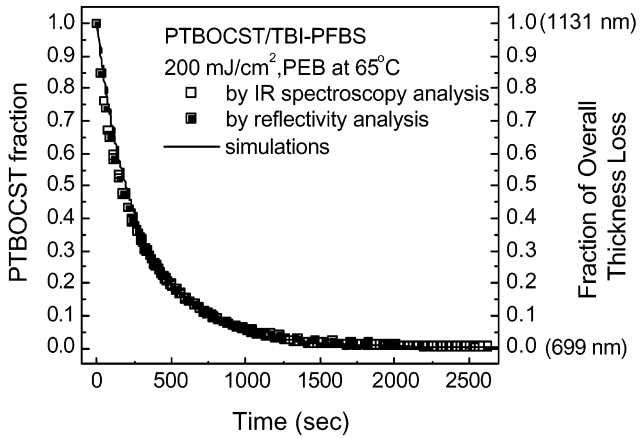

Figure 11. Comparison of the rates of deprotection as measured by infrared spectroscopy and the rates of film thickness loss as measured by spectroscopic reflectometry during heating of an exposed film of PTBOCST resist. CKS simulations of the thickness and PTBOCST fraction are overlaid on the experimental data.

nonvolatile deprotection side products. The NMR studies found that O-alkylation is favored under no- or low-acid conditions whereas C-alkylation is favored under high-acid conditions. This suggests that the new band is attributable, at least in part, to attack of *tert*-butyl species on the aryl ring.

Discussion

The data presented here provide a detailed view of the deprotection of PTBOCST polymer to form a PHOST-like material. The low-temperature decomposition pathway in the absence of acid is formation of an alkoxy species, with alkyl formation only becoming important during the autoaccelerated phase of polymer decomposition[13] around 170 °C. The presence of small amounts of acid promotes alkyl formation, whereas large amounts lead to deprotection via both the alkyl and alkoxy channels. Numerous secondary products are observed, their formation no doubt promoted by their high local density in the polymeric matrix. The chemistry can be described as an explosive process, using the classic definition of an explosion as a non-steady-state, rapid production of highly reactive molecules that are present in large concentrations and whose reactions dominate the decomposition process. Many of the products interact only weakly with the polymer, escaping rapidly into the gas phase as the polymer structure relaxes into its new, more dense state. A small percentage of the products attack the polymer chain, forming substituted poly(hydroxystyrene). The reactions observed are not anticipated from the thermolysis of the TBOCST monomer, which has much simpler chemistry.

These results have important implications in several areas. First, they provide definitive evidence that the commonly

TABLE 3: Results of Reflectance Analyses during PEB of CA Resist Films under Varying Conditions

resist polymer[a]	PEB temperature (°C)	exposure dose (mJ/cm^2)	effective half-life for thickness decrease[b]	upper limit transient free volume (%)
PTBOCST	65	200	200	<1
PTBOCST	85	200	7	<1
PTBOCST	100		0.5	~3
PTBOCST	100	2	8	<1
TBOCST/HOST[c]	85	200	8	<1

[a] All resist formulations contained 0.0445 m TBI-PFBS and were coated at initial thicknesses of ca. 1100 nm. [b] To facilitate comparison, an "effective half-life" is used here to characterize the time scale of a process; this is not intended to imply that that the kinetics of that process are first-order or that the form of the rate law is necessarily known. [c] Copolymer composition: TBOCST/HOST = 39:61.

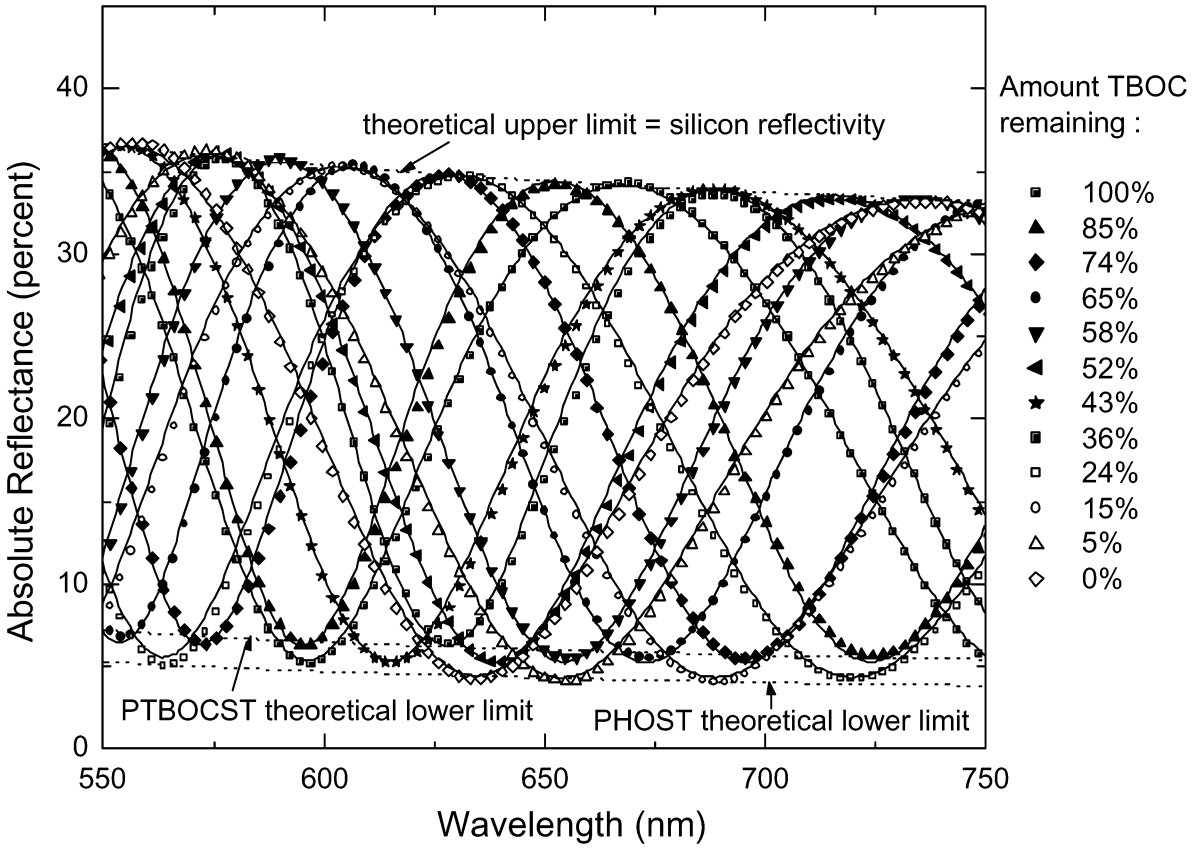

Figure 12. Comparison of reflectance spectra recorded during 65 °C PEB of exposed PTBOCST/TBI-PFBS resist with those predicted on the basis of the extent of deprotection.

accepted deprotection mechanism for PTBOCST polymer is incorrect: two decomposition channels are open, leading to alkoxy as well as alkyl products, and the final deprotected polymer is not pure PHOST. The earlier NMR studies and more recent MS investigations of homopolymers and copolymers with alkyloxycarbonyl protecting groups show that this general chemistry is common to a variety of resist materials.[3,36]

Second, the data presented here show that transient free volume plays little if any role in the acid diffusion process, countering the model that has been proposed elsewhere.[8,9] The mobility of ionic species in the resist is well-described as a classical diffusion process, sensitive to local environment and driven by a concentration gradient.[10] The agreement between simulations and experiment in linking the film thickness and the disappearance of PTBOCST confirms the results of other studies and shows that, even though the chemistry is complex, a simple description of it is sufficient to predict extents of reaction.[10,13,37] The kinetic model as currently structured does not provide insight into the microscopics of reactions, however. The abundance of mobile small molecules raises the question of exactly how acid moves through the polymer and what role, if any, these small molecules might play in the deprotection chemistry. Perfluorobutanesulfonic acid is a strong acid in the polymeric environment and, therefore, is essentially completely ionized. Acidolysis of the polymer involves trapping and release of protons, and protons must be bound to mobile species to move from pendant group to pendant group, particularly when the concentration of protecting groups is reduced. The role that deprotection products might play in this process is worth understanding: depending on their proton affinity, they might function as transfer agents or as proton traps, thus mediating the local availability of acid. Neutralization via proton transfer or electron capture can be expected to lead to distinct reaction paths, and understanding such details might provide insight into links between polymer composition and structure and the origin of resist sensitivity.

Finally, the fact that the deprotection products attack the resist polymer has implications for image development. The presence of substituents in the imaged regions of the polymer might locally alter the polymer reactivity and the permeability of the film to aqueous alkaline developer, thus affecting the formation of the final resist image. Studies of the reactive dissolution process should involve materials that allow this possibility to be tested explicitly.

Summary

Direct sampling using atmospheric-pressure mass spectrometry of gas streams from PTBOCST powders and films show that the deprotection involves two separate routes: elimination of *tert*-butoxy, the lowest-energy path, and elimination of *tert*-butyl. As its rate increases, the *tert*-butyl reaction appears to become intertwined with the *tert*-butoxy channel. The result is the formation of numerous small-molecule products, some of which desorb and are detected in the gas phase. This new view of the deprotection chemistry suggests that the nature of the catalytic chain activated during the PEB process in chemically amplified resists might be more complex than previously thought.

The relative rates of deprotection, product volatilization, and film densification have been assessed for PTBOCST resist films using a combination of IR spectroscopic analysis and high-speed spectroscopic reflectometry. These analyses indicate that, under conventional PEB process conditions, volatilization and densification are rapid compared to deprotection. Therefore, there is no substantial accumulation of volatile deprotection products

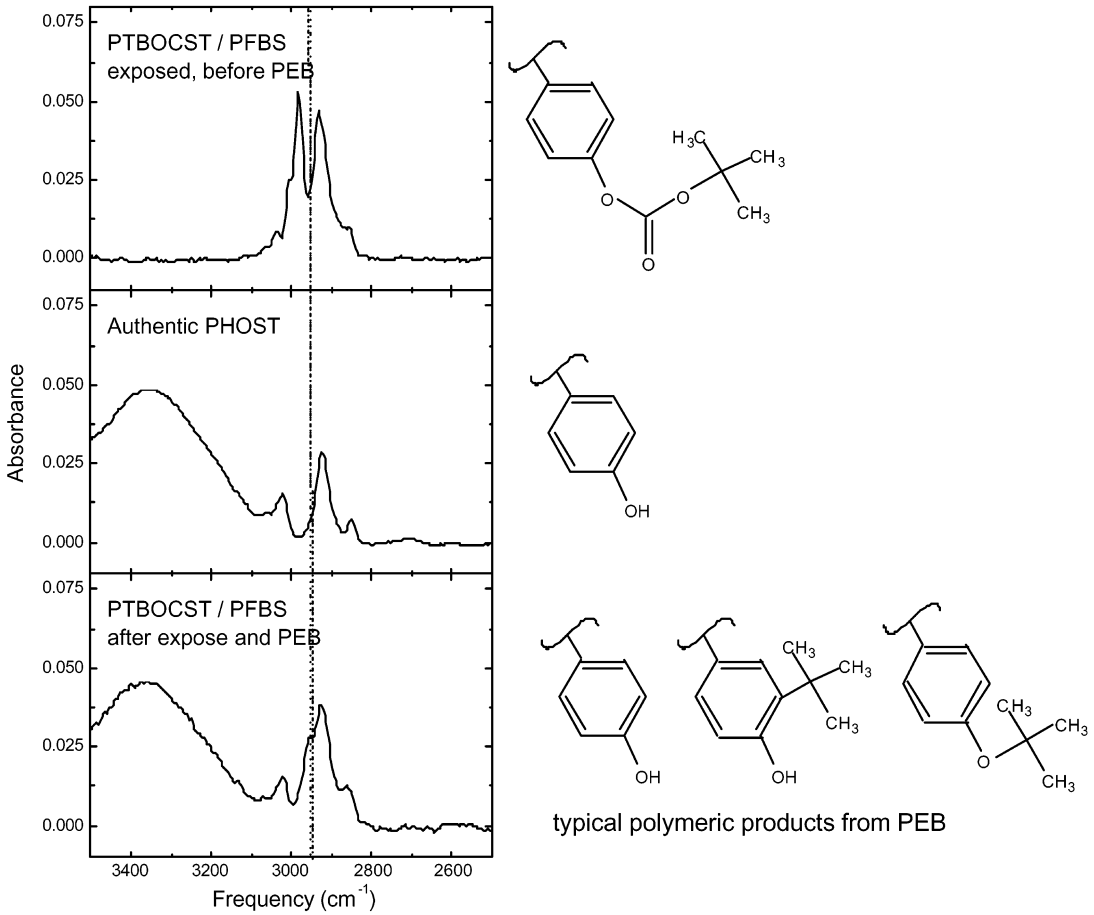

Figure 13. Infrared spectra illustrating the spectral differences between authentic PHOST and fully deprotected PTBOCST resist.

or excess free volume in the polymer film during normal PEB, evidence against these factors causing a significant transient enhancement in acid mobility during PEB. The implications of the data for resist imaging have been discussed.

Acknowledgment. This research was supported in part by the National Science Foundation Materials Research and Engineering Center Grant 9808677 to the Center for Polymer Interfaces and Macromolecular Assemblies. We are grateful to Greg Breyta for providing materials and to Greg Wallraff for helpful discussions.

References and Notes

(1) Thompson, L. F., Willson, C. G., Bowden, M. J., Eds. *Introduction to Microlithography*, 2nd ed.; American Chemical Society: Washington, DC, 1994.

(2) Kunz, R. R.; Downs, D. K. *J. Vac. Sci. Technol. B* **1999**, *17*, 3330.

(3) Ito, H.; Sherwood, M *Adv. Resist Technol. Process. XVI, Proc. SPIE—Int. Soc. Opt. Eng.* **1999**, *3678*, 104.

(4) Naylor, T. deV. *Comprehensive Polymer Science*; Allen, G., Bevington, J., Eds.; Pergamon Press: New York, 1989; Chapter 20.

(5) Nitzan, A.; Ratner, M. *J. Phys. Chem.* **1994**, *98*, 1764. Lonergan, M. C.; Nitzan, A.; Ratner, M. A.; Shriver, D. F. *J. Chem. Phys.* **1995**, *103*, 3253.

(6) Zuniga, M.; Wallraff, G.; Tomacruz, E.; Smith, B.; Larson, C.; Hinsberg, W.; Neureuther, A. *J. Vac. Sci. Technol. B* **1993**, *11*, 2862.

(7) Guillet, J. *Polymer Photophysics and Photochemistry*; Cambridge University Press: Cambridge, U.K., 1985; Chapter 3.

(8) Postnikov, S.; Stewart, M.; Tran, H.; Neirode, M.; Medeiros, D.; Cao, T.; Byers, J.; Webber, S.; Willson, C. G. *J. Vac. Sci. Technol. B* **1999**, *17*, 3335.

(9) Croffie, E.; Cheng, M.; Neureuther, A. *J. Vac. Sci. Technol. B* **1999**, *17*, 3339.

(10) Houle, F. A.; Hinsberg, W. D.; Morrison, M.; Sanchez, M. I.; Wallraff, G.; Larson, C.; Hoffnagle, J. *J. Vac. Sci. Technol. B* **2000**, *18*, 1874.

(11) Wallraff, G.; Hinsberg, W.; Houle, F. A.; Morrison, M.; Larson, C.; Sanchez, M.; Hoffnagle, J.; Brock, P.; Breyta, G. *Adv. Resist Technol. Process. XVI, Proc. SPIE—Int. Soc. Opt. Eng.* **1999**, *3678*, 138.

(12) After the completion of this work, our free-volume measurements were verified by Burns, S. D.; Stewart, M. D.; Hilfiker, J. N.; Synowicki, R. A.; Schmid, G. M.; Brodsky, C.; Willson, C. G. In *Forefront of Lithographic Materials Research, Proceedings of the 12th International Conference on Photopolymers*; Society of Plastics Engineers: Brookfield, CT, 2001; p 323. The PEB model described in refs 8 and 9 has recently been replaced by one very similar to that in ref 10; see: Schmid, G. M.; Smith, M. D.; Mack, C. A.; Singh, V. K.; Burns, S. D.; Willson, C. G. *Adv. Resist Technol. Process. XVIII, Proc. SPIE—Int. Soc. Opt. Eng.* **2001**, *4345*, 1037.

(13) Wallraff, G.; Hutchinson, J.; Hinsberg, W.; Houle F.; Seidel, P.; Johnson, R.; Oldham W. *J. Vac. Sci. Technol. B* **1994**, *12*, 3857.

(14) Frechet, J. M. J.; Eichler, E.; Ito, H.; Willson, C. G. *Polymer* **1983**, *24*, 995.

(15) Ito, H.; Ueda, M. *Macromolecules* **1988**, *21*, 1475.

(16) Houle, F. A.; Sanchez, M. I. IBM Almaden Research Center, San Jose, CA. Unpublished work, 2001.

(17) Preliminary reports of part of this work were presented in: Houle, F.; Poliskie, G.; Hinsberg, W.; Pearson, D.; Sanchez, M.; Ito, H.; Hoffnagle, J. *Adv. Resist Technol. Process. XVIII, Proc. SPIE—Int. Soc. Opt. Eng.* **2000**, *3999*, 181 and Hinsberg, W.; Houle, F.; Poliskie, M.; Pearson, D.; Sanchez, M.; Ito, H.; Hoffnagle, J.; Morrison, M. In *Forefront of Lithographic Materials Research, Proceedings of the 12th International Conference on Photopolymers*; Society of Plastics Engineers: Brookfield, CT, 2001; p 249.

(18) Breyta, G.; Dawson, D.; Ito, H.; Khojasteh, M.; Kwong, R. W.; Macy, E. H.; Merritt, D. P.; Moreau, W. M.; Pereault, S. E.; Sachdev, H. S.; Wood, R. L. U.S. Patent 6,153,696, Nov 28, 2000.

(19) Nguyen, C.; Carter, K.; Hawker, C.; Hedrick, J.; Jaffe, R.; Miller, R.; Remenar, J.; Rhee, H.; Rice, P.; Toney, M.; Trollsas, M.; Yoon, D. *Chem. Mater.* **1999**, *11*, 3080.

(20) Reid, N. M.; Buckley, J. A.; French, J. B.; Poon, C. C. *Adv. Mass Spectrom.* **1979**, *83*, 1843.

(21) Prime, R. B.; Shushan, B. *Anal. Chem.* **1989**, *61*, 1195 and references therein.

(22) Sunner, J.; Nicol, G.; Kebarle, P. *Anal. Chem.* **1988**, *60*, 1300; **1988**, *60*, 1308.

(23) McLafferty, F. W. *Interpretation of Mass Spectra*, 3rd ed.; University Science Books: Mill Valley, CA, 1980; Chapter 5.
(24) Houle F. A. *Int. J. Mass Spec. Ion Process*. **1993**, *123*, 243.
(25) McLafferty, F. W. *Interpretation of Mass Spectra*, 3rd ed.; University Science Books: Mill Valley, CA, 1980; Chapter 6.
(26) Born, M.; Wolf, E. *Principles of Optics*, 4th ed.; Pergamon Press: Oxford, U.K., 1970.
(27) Berning, J.; Berning, P. *J. Opt. Soc. Am.* **1960**, *50*, 813.
(28) Herman, I. *Optical Diagnostics for Thin Film Processing*; Academic Press: New York, 1996.
(29) Konnerth, K.; Dill, F. *IEEE Trans. Electron. Devices*, **1975**, *ED-22*, 452.
(30) Lauchlan, L.; Sautter, K.; Batchelder, T., Irwin, J. *Proc. SPIE* **1985**, *539*, 27.
(31) Metz, T.; Savage, R.; Simmons, H. *Proc. SPIE* **1991**, *1594*, 146.
(32) Aspnes, D. *Thin Solid Films*, **1982**, *89*, 249.
(33) Jellison Jr., G. *Thin Solid Films* **1993**, *234*, 416.
(34) Hinsberg, W. D.; Houle, F. A. *Chemical Kinetics Simulator*; IBM Almaden Research Center: San Jose, CA, 1996. Copies are available for downloading under a no-cost license from IBM at www.almaden.ibm.com/st/msim.
(35) Kochi, J. K. *Free Radicals*; Wiley: New York, 1973; Vol. II.
(36) Houle, F. A. IBM Almaden Research Center, San Jose, CA. Unpublished data, 2002.
(37) Houle, F. A.; Hinsberg, W. D.; Sanchez, M. I.; Hoffnagle, J. A. *J. Vac. Sci. Technol. B* **2002**, *20*, 924.